Composition-induced antiferroelectric phase and giant strain in lead-free $(Na_y,Bi_z)Ti_{1-x}O_{3(1-x)}$-$x$BaTiO$_3$ ceramics

Yiping Guo,[1,*] Mingyuan Gu,[1] Haosu Luo,[2] Yun Liu,[3] and Ray L. Withers[3]
[1]*State Key Laboratory of MMCs, Shanghai Jiaotong University, 200240 Shanghai, China*
[2]*Shanghai Institute of Ceramics, Chinese Academy of Science, 201800 Shanghai, China*
[3]*Research School of Chemistry, The Australian National University, Canberra ACT 0200, Australia*
(Received 10 November 2010; revised manuscript received 31 December 2010; published 28 February 2011)

$(Na_y,Bi_z)Ti_{1-x}O_{3(1-x)}$-$x$BaTiO$_3$ ceramics with an excess in Bi^{3+} and/or a deficiency in Na^+ were prepared and investigated. It is found that an antiferroelectric phase can be induced through a modulation of the mole ratio of Na^+ and Bi^{3+}. A phase boundary between ferroelectric and antiferroelectric phases can be observed at ambient temperature. A modulated phase, which is the origin of relaxor antiferroelectric behavior, should be attributed to a compositional modulation. The antiferroelectric phase can be induced to the ferroelectric phase by an applied electric field. The stability of the induced ferroelectric phase strongly depends on the mole ratio of Na^+ and Bi^{3+}. A recoverable giant strain of 0.48% comparable to $PbZrO_3$-based antiferroelectrics as well as electrostrictive coefficients (0.026 C^4 m^{-2}) much higher than lead-based relaxor ferroelectrics with low-temperature dependence was achieved in $(Na_y,Bi_z)Ti_{1-x}O_{3(1-x)}$-$x$BaTiO$_3$ antiferroelectrics. Our results show there is a high possibility that the novel lead-free antiferroelectrics will replace the $PbZrO_3$-based ones.

DOI: 10.1103/PhysRevB.83.054118 PACS number(s): 77.84.−s, 77.80.−e, 77.65.Bn, 77.22.Ej

I. INTRODUCTION

Antiferroelectrics (AFE's) have many potential applications in high-energy storage capacitors, high-strain actuators, pyroelectric sensors [for compositions near ferroelectric (FE) and AFE phase boundary], explosive electrical transducers, and electrical refrigeration.[1–11] Especially with the development of microelectronic devices, AFE thin films have huge applications in microelectromechanical systems (MEMS) and decoupling capacitors in high-speed dynamic random access memory (DRAM) devices.[12–14] However, there are only a few functional oxides that exhibit antipolar cation displacements that can be fabricated at ambient pressures. And until now, only $PbZrO_3$-based compounds have ever shown the ability to switch between an antipolar (AFE) and polar (FE) state under electric field, giving rise to large strain and/or charge. Thus, $PbZrO_3$-based AFE materials have been extensively studied over the past several decades.[1–14] However, a restriction of PbO use in electronic devices is now demanded by environmental legislation in the European Union and part of Asia.[15] The discovery of a new kind of PbO-free AFE compound is therefore extremely urgent from the fundamental scientific perspective and from a device application standpoint.

The $(1-x)(Na_{0.5}Bi_{0.5})TiO_3$-$x$BaTiO$_3$ [abbreviated as NBT-BT $100(1-x)/100x$ hereafter] system is made up of well-known lead-free piezoelectric materials.[15–19] They show AFE behavior at a temperature depending on the BT content. For pure NBT, the depolarization temperature (T_d), that is, the transition temperature from the FE to the AFE phase, is at about 190 °C. For compositions at the morphotropic phase boundary (MPB) ($x \approx 0.06$–0.08), T_d decreases to about 100 °C. When the BT content is increased further, the T_d will increase again. With regard to the origin of AFE behavior in the NBT system, Dorect *et al.* reported that the low-temperature FE rhombohedral to higher-temperature tetragonal phase transition in NBT is a two-step phase-transition process via an AFE-like, intermediate modulated phase, which is typically revealed from the occurrence of $G \pm 1/2\langle 110\rangle_p^*$ superstructure spots and their elongation along $\langle 001\rangle_p^*$ over the 200–320 °C temperature range.[20,21] The formation of this modulated phase was proposed to be responsible for the AFE and relaxor-like behavior in NBT observed over the 200–320 °C temperature range.[20,21] Very recently, Ma *et al.* proposed an additional phase region exhibiting *P4bm* nanodomains ($0.07 \leqslant x \leqslant 0.09$). A new concept "relaxor AFE" was used to describe the unique short-range AFE order.[22] Obviously, the origin of AFE behavior is still the point at issue. In previous studies,[15–19] the mole ratio of Na^+ and Bi^{3+} was always considered to be 1 due to the contrasting valence of the two involved cations (+1 for Na and +3 for Bi). However, it is in fact hard to keep the 1 : 1 ratio due to volatilization of Bi_2O_3 and Na_2O during sintering, which can lead to the variation of piezoelectric properties and depolarization temperatures in the published data.[14–19] Therefore, the effect of Na^+ or Bi^{3+} nonstoichiometry on the structure and properties should not be ignored. There have been several previous studies concerning the nonstoichiometry issue of NBT-BT ceramics[23–26] involving Na^+ or Bi^{3+} nonstoichiometry. They found that T_d will decrease with an excess in Bi^{3+} or a deficiency in Na^+.[23,26] The specimens with high excess Bi^{3+} in NBT-BT 93/7 ceramics present shrunk and deformed hysteresis loops at room temperature. Xu *et al.* attributed the observed behavior to the generation of AFE microregions in the macroscopic FE matrices.[23] It is evident that the appearance of the AFE phase is strongly related to the mole ratio of Na^+ and Bi^{3+}. We therefore conducted a systematic investigation on NBT-BT ceramics with a deficiency in Na^+ and/or an excess in Bi^{3+}.

In this paper, it is found that the AFE phase can be induced at ambient temperature through a compositional modulation of Na^+ and Bi^{3+} in a lead-free $(Na_y,Bi_z)Ti_{1-x}O_{3(1-x)}$-$x$BaTiO$_3$ (abbreviated as $N_{100y}B_{100z}T_{100(1-x)}$-$100x$BT hereafter) system at ambient temperature. The AFE ceramics show the ability to switch between an antipolar (AFE) and a polar (FE) state under electric field as occurs in $PbZrO_3$-based ceramics. The stability

of the induced FE phase strongly depends on the mole ratio of Na^+ and Bi^{3+}. Giant electric-induced strain and a notably larger electrostrictive coefficient were thereby achieved.

II. EXPERIMENTAL

Ceramics with nominal composition $N_{100y}B_{100z}T_{100(1-x)}$-$100x$BT ($x = 0$, 0.06, 0.07, 0.08, 0.12, and 0.15, $y = 0.395$–0.500, $z = 0.400$–0.515) were synthesized using the solid-state reaction method. High-purity Na_2CO_3, Bi_2O_3, $BaCO_3$, and nano-TiO_2 (~20 nm) were used as starting materials. Mixtures of these starting materials in the appropriate ratio were first ball-milled for 12 h using ethanol as a medium followed by an initial calcination at 800 °C for 2 h. The calcined powder was then ball-milled again for 12 h and dried, followed by the addition of poly(vinylalcohol) as a binder. The resultant powder was then granulated and pressed into pellets with a diameter of 13 mm under a uniaxial pressure of 200 MPa. Finally, these pellets were sintered in air at 1150 °C for 2 h in a covered alumina crucible.

X-ray diffraction (XRD) measurements were performed on as-sintered ceramics surfaces with a BRUKER-AXS x-ray diffractometer with monochromatic Cu $K\alpha$ radiation in the step scanning mode with increments of 0.05°. For transmission electron microscopy (TEM) observation, as-sintered samples were mechanically polished down to 5 μm and then Ar-ion

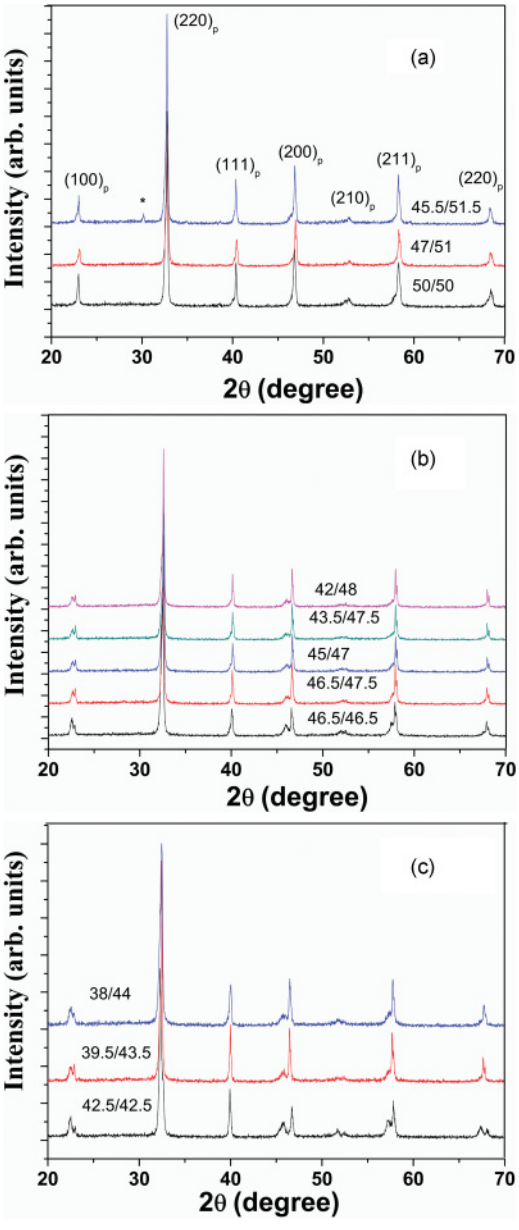

FIG. 1. (Color online) X-ray diffraction patterns of $N_{100y}B_{100z}T_{100(1-x)}$-$x$BT samples ($100y/100z$), in which the diffraction peaks were indexed according to the perovskite parent structure: (a) for $N_{100y}B_{100z}T_{100}$ ceramics, the peak with an asterisk corresponding to a second phase; (b) for $N_{100y}B_{100z}T_{93}$-7BT ceramics; and (c) for $N_{100y}B_{100z}T_{85}$-15BT ceramics.

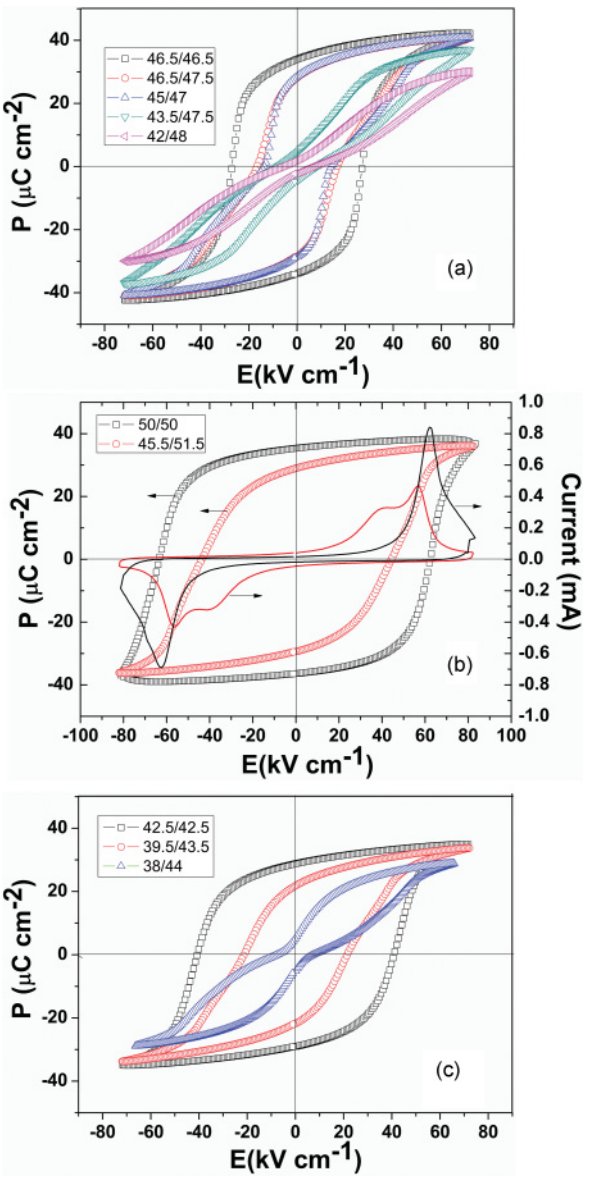

FIG. 2. (Color online) Hysteresis loops for (a) $N_{100y}B_{100z}T_{93}$-7BT samples; hysteresis loops and associated *I-V* curves for (b) $N_{100y}B_{100z}T_{100}$ samples and (c) $N_{100y}B_{100z}T_{85}$-15BT samples. The frequency of applied alternating current (ac) electrical fields is 1 Hz.

milled to electron transparency. TEM studies were carried out on a JEM-2010/INCA OXFORD microscope operated at 200 kV.

For electrical characterization, the resultant samples were coated with silver paste on their surfaces and heat treated at 500 °C for 5 min to ensure good electrical contact. The polarization-field (*P-E*) and strain-field (*S-E*) hysteresis loops as well as the associated switching current (*I-V*) behavior were investigated by using an aixACCT FE test unit in conjunction with a laser interferometer. The samples were immersed in silicone oil to prevent arcing during the measurement. After unipolar strain characterization at room temperature, the dielectric properties were measured by using a computer-controlled Agilent 4294A impedance analyzer.

III. RESULTS AND DISCUSSION

The present study started with a series of $N_{100y}B_{100z}T_{100(1-x)}-100x$BT ceramics. The XRD patterns of $N_{100y}B_{100z}T_{100}$, $N_{100y}B_{100z}T_{93}$-7BT, and $N_{100y}B_{100z}T_{85}$-15BT are shown in Figs. 1(a)–1(c), respectively. Indexation is with respect to the underlying parent perovskite substructure (labeled with the subscript p, which denotes parent in what follows). Almost all the resultant ceramics can be identified as having a perovskite type structure except that of the $N_{45.5}B_{51.5}T_{100}$ ceramics. For pure $N_{100y}B_{100z}T_{100}$ ceramics, they all show rhombohedral symmetry, but an asymmetry of the $(200)_p$ peak was found for ceramics with a higher excess in Bi^{3+} and/or a higher deficiency in Na^+ (indicative of pseudorhombohedral symmetry). For $N_{100y}B_{100z}T_{100(1-x)}-100x$BT ceramics with $x = 0.06$, 0.07, and 0.08, no significant change in phase structure was found for ceramics with an excess in Bi^{3+} and/or a deficiency in Na^+. Noticeable broadening of the $(111)_p$ peak and splitting of the $(200)_p$ peak were detected for all samples. This means that the ceramics with an excess in Bi^{3+} and/or a deficiency in Na^+ still show the coexistence of rhombohedral and tetragonal phases, that is, they are still in the MPB region. For $N_{100y}B_{100z}T_{100(1-x)}-100x$BT ceramics with $x = 0.12$ and 0.15, the $(111)_p$ peak is not split while the $(200)_p$ peak clearly splits, which is indicative of tetragonal symmetry. The specimens with an excess in Bi^{3+} and/or a deficiency in Na^+ still maintain tetragonal symmetry. But note that the relative intensity of the $(002)_p$ peak become weaker and shifts to a higher angle.

The *P-E* behavior for the $N_{100y}B_{100z}T_{93}$-7BT ceramics are shown in Fig. 2(a). For $N_{46.5}B_{46.5}T_{93}$-7BT samples, *P-E* loops appear to exhibit a typical *P-E* ferroelectric hysteresis loop character. With a smaller excess in Bi^{3+}, pinched *P-E* hysteresis loops were observed in the specimens at ambient temperature as observed by Xu *et al.*[23] For specimens with a higher excess in Bi^{3+} and/or a deficiency in Na^+, typical AFE double hysteresis loops were observed at ambient temperature ($100y/100z$: 43.5/47.5 and 42/48). Our findings demonstrate that the AFE polarization phase only exists in $N_{100y}B_{100z}T_{93}$-7BT specimens with a higher excess in Bi^{3+} and/or a deficiency in Na^+. The AFE phase can be induced to the FE phase. However, the induced FE phase is unstable, as is that in $PbZrO_3$. They will return to the AFE phase after removing the electric field. Therefore, the appearance of pinched hysteresis loops clearly shows that a metastable FE phase can coexist with the AFE phase in the poled samples. Note that the appearance of the metastable FE phase has two possible explanations. One is that the metastable FE phase

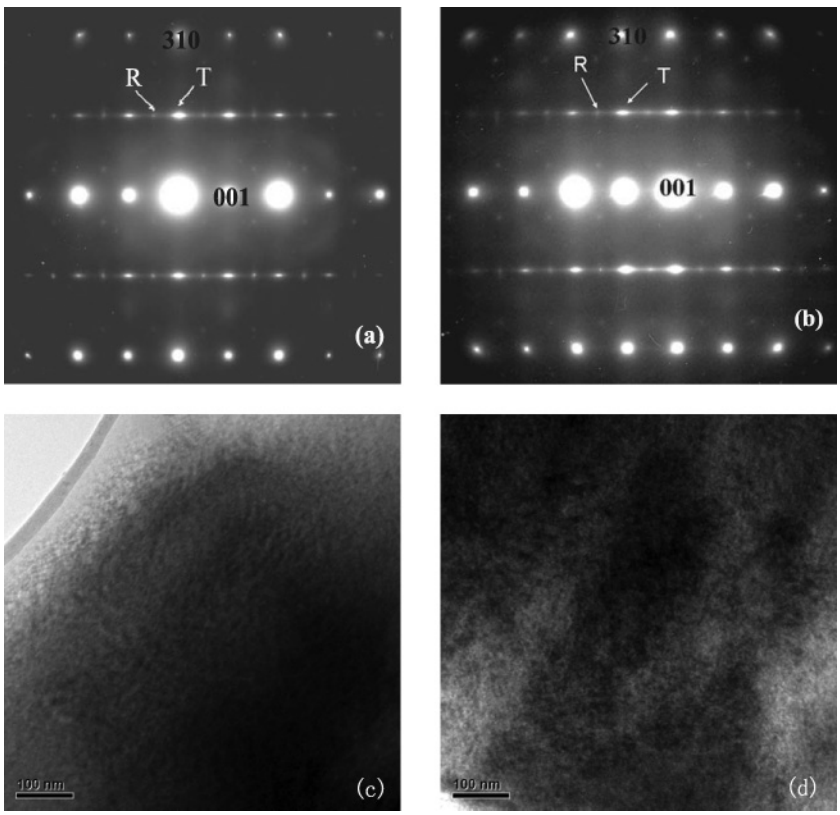

FIG. 3. Electron diffraction patterns of unpoled $N_{100y}B_{100z}T_{93}$-7BT samples collected along the $\langle 310\rangle_p$ zone axis for (a) $N_{46.5}B_{46.5}T_{93}$-7BT and (b) $N_{43.5}B_{47.5}T_{93}$-7BT. The $G \pm {}^1/_2\langle 111\rangle_p^*$ reflections are labeled *R* while the $G \pm {}^1/_2\langle 110\rangle_p^*$ spots are labeled *T*. TEM images of unpoled $N_{100y}B_{100z}T_{93}$-7BT samples collected along the $\langle 011\rangle_p$ zone axis for (c) $N_{46.5}B_{46.5}T_{93}$-7BT and (d) $N_{43.5}B_{47.5}T_{93}$-7BT.

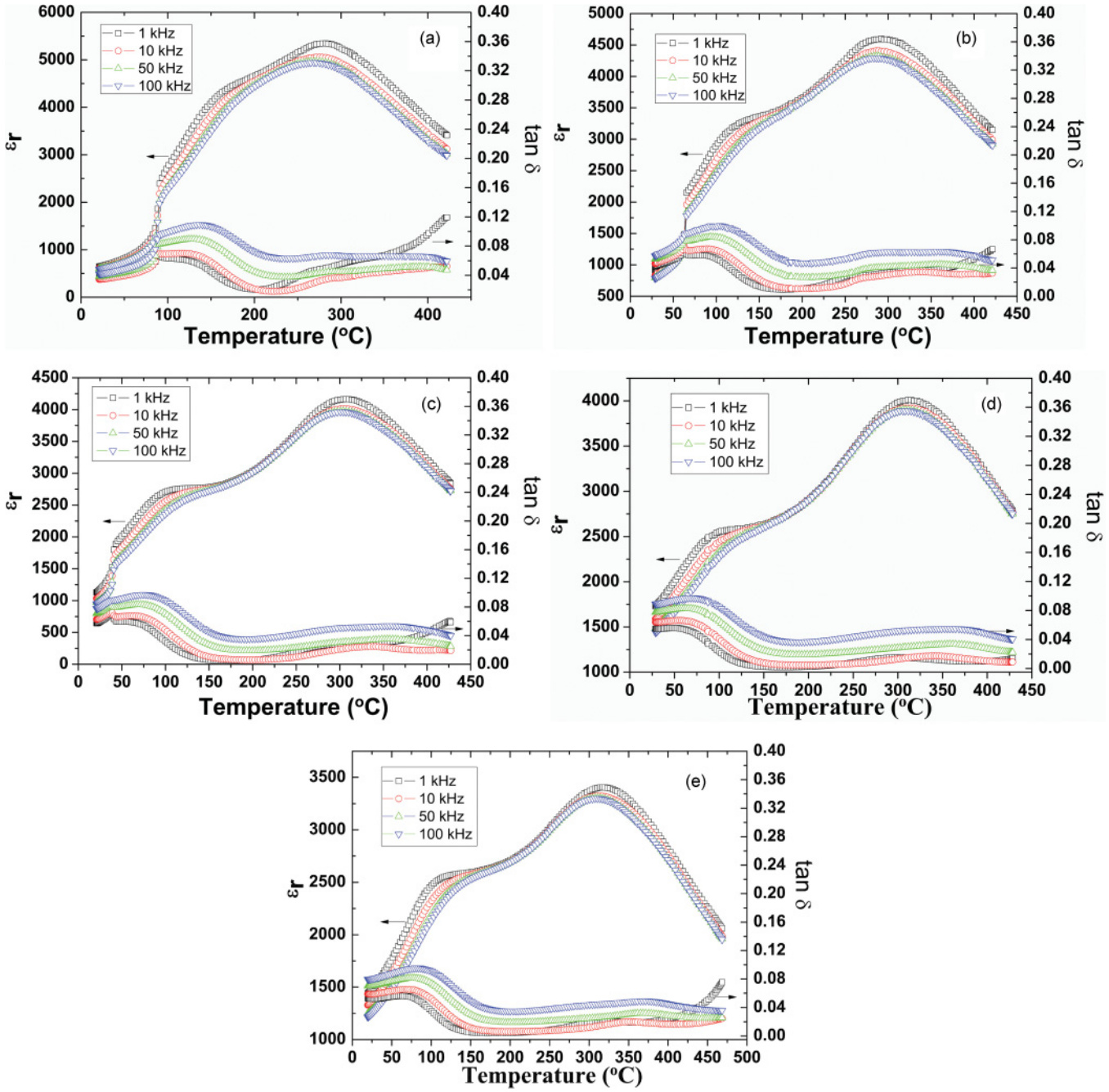

FIG. 4. (Color online) Temperature- and frequency-dependent dielectric constant and loss tangent of poled $N_{100y}B_{100z}T_{94}$-6BT samples: (a) $N_{47}B_{47}T_{94}$-6BT, (b) $N_{45.5}B_{47.5}T_{94}$-6BT, (c) $N_{44}B_{47}T_{94}$-6BT, (d) $N_{44}B_{48}T_{94}$-6BT, and $N_{42.5}B_{48.5}T_{94}$-6BT.

coexists with the AFE phase in the unpoled $N_{100y}B_{100z}T_{93}$-7BT samples. The other is that the AFE phase only exists in the unpoled $N_{100y}B_{100z}T_{93}$-7BT samples, the metastable FE phase is induced from the AFE phase, and the induced FE phase will partially return to the AFE phase after removing the electric field. To clarify this point, electron diffraction (ED) patterns at the $\langle 310\rangle_p$ zone axis for $N_{46.5}B_{46.5}T_{93}$-7BT with typical FE hysteresis loop character and $N_{43.5}B_{47.5}T_{93}$-7BT with typical AFE hysteresis loop character were investigated, as shown in Figs. 3(a) and 3(b), respectively. The ED patterns display $G \pm {}^1/_2\langle 111\rangle_p^*$ superstructure reflections (R type) from the rhombohedral phase as well as $G \pm {}^1/_2\langle 110\rangle_p^*$ reflections (T type) from the tetragonal phase, which means a coexistence of rhombohedral and tetragonal phases. A strong stretching of the $G \pm {}^1/_2\langle 110\rangle_p^*$ reflections and diffuse streak lines parallel to $\langle 001\rangle_p^*$ were found at room temperature in all two samples. This can only be clearly observed in the temperature range between 200 and 320 °C in pure NBT ceramics (cf. with Fig. 4 in Ref. 20). In this temperature range, a periodic distribution of *Pnma* orthorhombic perovskite sheets, with their own octahedral tilting system, developed as an intergrowth within the *R3C* rhombohedral matrix, in which the formation of *Pnma* sheets can be easily achieved as it represents natural $\{100\}_p$ twin planes separating two

R3C FE domains related by a pseudomerohedral twinning law.[20] A modulated phase is formed of *Pnma* orthorhombic sheets, appearing within the *R3C* parental matrix and exhibiting $a^-a^+a^-$ octahedral tilting system.[20] Similarly, such a modulated phase, which was proposed to be the origin of relaxor AFE behavior in pure NBT by Dorcet *et al.*,[20] should also exist in $N_{100y}B_{100z}T_{93}$-7BT ceramics at ambient temperature. It is also observed that the $G \pm 1/2\langle 110\rangle_p^*$ spots are more stretched in unpoled $N_{43.5}B_{47.5}T_{93}$-7BT samples than those of $N_{46.5}B_{46.5}T_{93}$-7BT samples. We then may propose that the amount of modulated phase is correlated with the stretching degree of the $G \pm 1/2\langle 110\rangle_p^*$spots. The stretching degree may increase with more excess in Bi^{3+} and deficiency in Na^+. The TEM results from representative grains in these two ceramics are shown in Figs. 3(c) and 3(d), respectively. Nanodomains were observed as the results of Ma *et al.* The size of nanodomains in $N_{46.5}B_{46.5}T_{93}$-7BT is slightly larger than that in $N_{43.5}B_{47.5}T_{93}$-7BT, which is consistent with the relaxor AFE character for these two samples. Therefore, as proposed by Ma *et al.* very recently,[22] the MPB region may be an AFE phase region. The AFE phase can be induced to the FE phase and the induced FE phase can exist stably after removing the electric field in $N_{46.5}B_{46.5}T_{93}$-7BT samples as occurs in (Pb,La)(Zr,Sn,Ti)O_3.[11,12] However, the induced FE phase will partially return to the AFE phase after removing the electric field in $N_{46.5}B_{47.5}T_{93}$-7BT samples. The above results demonstrate that the stability of the induced FE phase for ceramics in the MPB region can be tailored through the compositional modulation of Na^+ and Bi^{3+}. In addition to the AFE phase that exists in the MPB region, we found that pinched as well as double hysteresis loops can also be observed for compositions away from the MPB region with a higher excess in Bi^{3+} and/or a deficiency in Na^+ with $x = 0$, 0.12, and 0.15. The hysteresis loops and associated *I-V* curves for $N_{50}B_{50}T_{100}$ are shown in Fig. 2(b); AFE behavior can be clearly seen in the corresponding switching current curve. The hysteresis loops for $N_{100y}B_{100z}T_{85}$-15BT samples are shown in Fig. 2(c); a double hysteresis loop can be clearly observed for $N_{38}B_{44}T_{100}$-15BT samples. The $N_{50}B_{50}T_{100}$ and $N_{42.5}B_{42.5}T_{85}$-15BT samples are well accepted as a rhombohedral FE phase with *R3c* space group and a tetragonal FE phase with *P4mm* space group, respectively. Therefore, a pure AFE phase or the coexistence of FE and AFE phases in the ground state is proposed for compositions away from the MPB with a higher excess in Bi^{3+} and/or a deficiency in Na^+, that is, there are phase boundaries between FE and AFE phases in the compositions away from the MPB region. ED patterns at the $\langle 310\rangle_p$ zone axis for the two unpoled samples also show a strong stretching of the $G \pm 1/2\langle 110\rangle_p^*$ reflections and diffuse streak lines parallel to $\langle 001\rangle_p^*$ at room temperature. Then we speculated that a modulated phase, which has been proposed to be the origin of relaxor AFE behavior, can be developed not only within the *R3c* parent matrix but also within the *P4mm* parent matrix. Dorcet *et al.* proposed that the modulated phase better corresponds to a strain modulation rather than to a compositional modulation.[20] Our results show that the modulated phase may be due to a compositional modulation, although such a phenomenon seems impossible due to the contrasting valence of the two involved cations (+1 for Na and +3 for Bi).

To further investigate the phase-transition behavior, the temperature dependence of the relative dielectric permittivity ε_r and loss tangent $\tan\delta$ for poled $N_{100y}B_{100z}T_{100(1-x)} - xBT$ samples was measured. Figures 4(a)–4(e) show the temperature dependence of the relative dielectric permittivity ε_r and loss tangent $\tan\delta$ for poled $N_{100y}B_{100z}T_{94} - 6BT$ samples. For $N_{47}B_{47}T_{94}$-6BT, $N_{45.5}B_{47.5}T_{94}$-6BT, and $N_{44}B_{47}T_{93}$-7BT samples, the inflection point of $\tan\delta$ observed at lower temperature is T_d, corresponding to the FE-AFE phase transition. Note that T_d decreases for specimens with more excess in Bi^{3+} and/or more deficiency in Na^+. The T_d for $N_{47}B_{47}T_{94}$-6BT, $N_{45.5}B_{47.5}T_{94}$-6BT, and $N_{44}B_{47}T_{93}$-7BT samples are 88, 66, and 38°C (1 kHz), respectively. The frequency dispersion in ε_r and $\tan\delta$ is weaker at temperatures below T_d but becomes significant above T_d. The frequency dispersion in ε_r and $\tan\delta$ is a minimum at a temperature below T_d for $N_{47}B_{47}T_{94}$-6BT and gradually becomes stronger for specimens with more excess in Bi^{3+} and/or more deficiency in Na^+. These results further confirm that the stability of the induced FE phase strongly depends on the mole ratio of Bi^{3+} and Na^+. With further increase in temperature, the frequency dispersion becomes weaker or even vanishes before reaching T_m (the temperature where ε_r reaches a maximum) with more excess in Bi^{3+} and/or more deficiency in Na^+. In contrast to the above three compositions, for $N_{44}B_{48}T_{94}$-6BT and $N_{42.5}B_{48.5}T_{94}$-6BT samples, no sharp anomaly exists in either the ε_r versus T or the $\tan\delta$ versus T curve at lower temperature, that is, we cannot observe the T_d anymore. The frequency-dependent ε_r and $\tan\delta$ show typical relaxor characteristics until the relaxor behavior vanishes at a temperature higher than 150 °C. This dielectric behavior coincides well with short-range AFE order. The dielectric behaviors of other ceramics were also measured. Similar dielectric dispersion behaviors were observed in all the samples.

It is well known that a large electric-field-induced strain can be achieved associated with the AFE-FE phase transition. We also measured the electric-field-induced strain for the $N_{100y}B_{100z}T_{100(1-x)}-100x$BT samples. Typical strain field (*S-E*) curves of AFE's were observed in $N_{100y}B_{100z}T_{100(1-x)}-100x$BT ceramics with a higher excess in Bi^{3+} and/or a deficiency in Na^+ (without negative strain). A giant recoverable strain of 0.48% under 70 kV/cm was achieved in the $N_{44}B_{48}T_{94}$-6BT sample (Fig. 5). This value

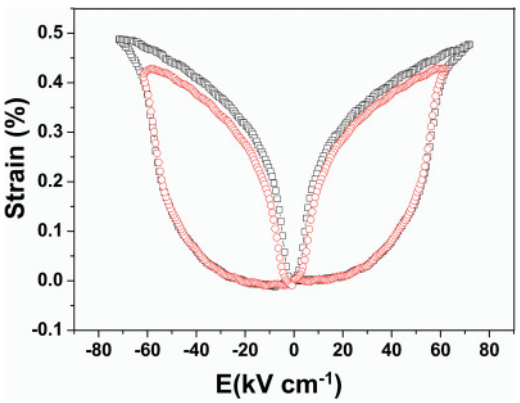

FIG. 5. (Color online) Bipolar strains of $N_{44}B_{48}T_{94}$-6BT samples measured under an electrical field with a frequency of 1 Hz.

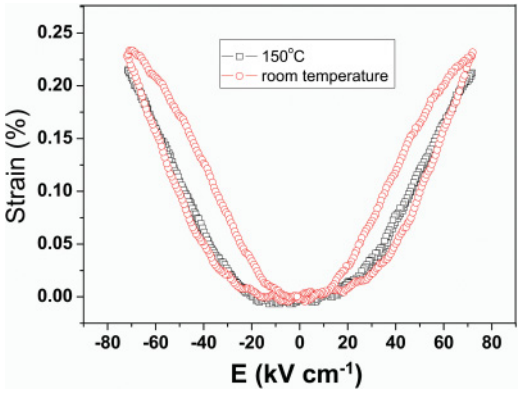

FIG. 6. (Color online) Bipolar strains of $N_{42}B_{48}T_{93}$-7BT samples measured under an electrical field with a frequency of 1 Hz at room temperature and 150 °C.

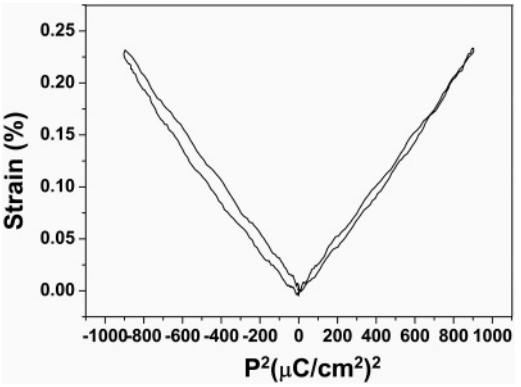

FIG. 7. S-P^2 curves of the $N_{42}B_{48}T_{93}$-7BT samples, indicating electrostrictive effect.

is higher than all the recently reported NBT-based ceramics and even higher than the strain obtained with established FE $Pb(Zr,Ti)O_3$ ceramics.[27–32] A strain of 0.23% with small hysteresis under 70 kV/cm at room temperature was obtained in the $N_{42}B_{48}T_{93}$-7BT sample (Fig. 6). This value is comparable to strains obtained in Pb-based AFE's. Figure 7 shows the plots of S and P^2 derived from the room temperature S-E curve of Fig. 6. The slope of this curve corresponds to the electrostriction coefficient.[28] Clearly, the S-P^2 curves deviate slightly from linear relations, which means the contribution of electrostriction strain should be predominant. The averaged electrostrictive coefficient (Q) is calculated to be of 0.026 m^4 C^{-2}. This value is comparable to the recently reported NBT-BT-$(Na,K)NaO_3$ ceramics and much higher than the lead-based electrostrictive material [for $Pb(Mg_{1/3}Nb_{2/3})$-$PbTiO_3$, Q is reported to be about 0.017 m^4 C^{-2} (Ref. 33)]. Moreover, a strain of 0.21% with no hysteresis is still available when the temperature is up to 150 °C (Fig. 6). All these results demonstrate that $N_{42}B_{48}T_{93}$-7BT ceramics are suitable for high-precision positioning devices and actuators. New insight has also been provided into ways to further optimize lead-free AFE electrostrictors.

IV. CONCLUSIONS

The ground state is an AFE phase at ambient temperature for unpoled compositions in the MPB region. The ground state of the ceramics shows the coexistence of AFE and FE phases or a pure AFE phase for unpoled compositions away from the MPB region with a high excess in Bi^{3+} and/or a high deficiency in Na^+, that is, there are phase boundaries between FE and AFE phases at ambient temperature at these compositions. The AFE $N_{100y}B_{100z}T_{100(1-x)}-100x$BT ceramics shows the ability to switch between an antipolar (AFE) and a polar (FE) state under electric field as occurs in $PbZrO_3$-based ceramics. The stability of the induced FE phase strongly depends on the mole ratio of Na^+ and Bi^{3+}. A recoverable giant strain of 0.48% or electrostrictive coefficients as high as 0.026 m^4 C^{-2} (about 1.5 times the value of traditional Pb-based electrostrictors) has been observed in $N_{100y}B_{100z}T_{100(1-x)}-100x$BT AFE ceramics. Our results show that these lead-free AFE's have huge application potential for use as sensors and actuators.

ACKNOWLEDGMENTS

This work is supported by the Pujiang Scholar Foundation of Shanghai, China (Grant No. 08PJ1407100), the Natural Science Foundation of China (Grant No.11074165) and the Australian Research Council Discovery Program.

*ypguo@sjtu.edu.cn

[1] C. H. Peng and S. B. Desu, Appl. Phys. Lett. **61**, 16 (1992).
[2] C. A. Paz de Araujo, J. D. Cuchiaro, L. D. Mcmillan, M. C. Scott, and J. F. Scott, Nature (London) **374**, 627 (1995).
[3] D. Berlinecourt, H. Jaffe, H. H. A. Krueger, and B. Jaffe, Appl. Phys. Lett. **3**, 90 (1963).
[4] W. Y. Pan, C. Q. Dam, Q. M. Zhang, and R. E. Cross, J. Appl. Phys. **66**, 6014 (1989).
[5] G. H. Haertiling, J. Am. Ceram. Soc. **82**, 797 (1999).
[6] W. Mock and W. H. Holt, J. Appl. Phys. **49**, 846 (1978).
[7] Y. L. Wang and W. Z. Yuen, Ferroelectrics **49**, 169 (1982).
[8] C. Heremans and H. L. Tuller, J. Appl. Phys. **87**, 1458 (2000).
[9] W.-H. Chan, Z. Xu, J. Zhai, and H. Chen, Appl. Phys. Lett. **87**, 192904 (2005).
[10] A. S. Mischenko, Q. Zhang, J. F. Scott, R. W. Whatmore, and N. D. Mathur, Science **311**, 1270 (2006).
[11] S. S. N. Bharadwajia and S. B. Krupanidhi, Ferroelectrics **263**, 39 (2001).
[12] X. Y. Zhang, X. Zhao, C. W. Lai, J. Wang, X. G. Tang, and J. Y. Dai, Appl. Phys. Lett. **85**, 4190 (2004).
[13] D. L. Polla and L. F. Francis, MRS Bull. **21**, 56 (1996).
[14] I. W. Kim, D. S. Lee, S. H. Kang, and C. W. Ahn, Thin Solid Films **441**, 115 (2003).
[15] C. Xu, D. Lin, and K. W. Kwok, Solid State Sci. **10**, 934 (2008).
[16] M. Chen, Q. Xu, B. H. Kim, B. K. Ahm, J. H. Ko, W. J. Kang, and O. J. Nam, J. Eur. Ceram. Soc. **28**, 843 (2008).
[17] B. J. Chu, D. R. Chen, G. R. Li, and Q R. Yin, J. Eur. Ceram. Soc. **22**, 2115 (2002).

[18]T. Takenaka, K. Maruyama, and K. Sakata, Jpn. J. Appl. Phys. **30**, 2236 (1991).
[19]J. Rödel, W. Jo, K. T. P. Seifert, E.-M. Anton, and T. Granzow, J. Amer. Ceram. Soc. **92**, 1153 (2009).
[20]V. Dorcet, G. Trolliard, and P. Boullay, Chem. Mater. **20**, 5061 (2008).
[21]V. Dorcet, G. Trolliard, and P. Boullay, J. Magn. Magn. Mater. **321**, 1758 (2009).
[22]C. Ma and X. Tan, Solid State Commun. **150**, 1497 (2010).
[23]Q. Xu, D.-P. Huang, M. Chen, W. Chen, H.-X. Liu, and B.-H. Kim, J. Alloys Compd. **471**, 310 (2009).
[24]S. E. Park, S. J. Chung, I. T. Kim, and K. S. Hong, J. Am. Ceram. Soc. **77**, 2641 (1994).
[25]S. E. Park, S. J. Chung, and I. T. Kim, J. Am. Ceram. Soc. **79**, 1290 (1996).
[26]Y. S. Sung, J. M. Kim, J. H. Cho, T. K. Song, M. H. Kim, H. H. Chong, T. G. Park, D. Do, and S. S. Kim, Appl. Phys. Lett. **96**, 022901 (2010).
[27]C. Ma and X. Tan, Solid State Commun. **150**, 1497 (2010).
[28]S. Zhang, A. B. Kounga, W. Jo, C. Jamin, K. Seifert, T. Granzow, J. Rödel, and D. Damjanovic, Adv. Mater. **21**, 4716 (2009).
[29]S. Zhang, A. B. Kounga, E. Aulbach, and Y. Deng, J. Am. Ceram. Soc. **91**, 3950 (2008).
[30]S. Zhang, A. B. Kounga, E. Aulbach, H. Ehrenberg, and J. Rödel, Appl. Phys. Lett. **91**, 112906 (2007).
[31]S. Zhang, A. B. Kounga, E. Aulbach, T. Granzow, W. Jo, H.-J. Kleebe, and J. Rödel, J. Appl. Phys. **103**, 034107 (2008).
[32]Y. Hiruma, Y. Imai, Y. Watanabe, H. Nagata, and T. Takenaka, Appl. Phys. Lett. **92**, 262904 (2008).
[33]A. B. Kounga, S. Zhang, W. Jo, T. Granzow, and J. Rödel, Appl. Phys. Lett. **92**, 222902 (2008).